Critical behavior and universality in gravitational collapse of a charged scalar field

Shahar Hod and Tsvi Piran
The Racah Institute for Physics, The Hebrew University, Jerusalem, 91904 Israel
(Received 1 July 1996)

We summarize results from a study of spherically symmetric collapse of a *charged* (complex) massless scalar field. We present an analytic argument which conjectures the generalization of the mass-scaling relation and echoing phenomena, originally discovered by Choptuik, for the *charged* case. Furthermore, we study the behavior of the self-similar critical solution under *external* perturbations — addition of a cosmological constant Λ and under a variation of the charge coupling constant e. Finally, we study the scaling relation of the black-hole charge. Using an analytic argument, we conjecture that black holes of infinitesimal mass are neutral or obey the relation $Q_{\rm BH} \ll M_{\rm BH}$. We verify our predictions with numerical results. [S0556-2821(97)00106-9]

PACS number(s): 04.40.Nr, 04.70.Bw

I. INTRODUCTION

Gravitational collapse is one of the most interesting phenomena in general relativity. The dynamics of a spherically symmetric massless scalar field [1] coupled to general relativity has two kinds of possible end states. Either the scalar field eventually dissipates away leaving spacetime flat or a black-hole forms. Numerical simulations of this model problem [2] have revealed a very interesting phenomena — a kind of critical behavior which is a feature of supercritical initial conditions very close to the critical case $p=p^*$ (p is a parameter which characterizes the strength of the initial configuration, and p^* is the threshold value). More precisely, Choptuik found a power-law dependence of the black-hole mass on critical separation $p-p^*$ of the form

$$M_{\rm BH} \propto \begin{cases} 0, & p \leqslant p^*, \\ (p-p^*)^{\beta}, & p > p^*. \end{cases} \tag{1}$$

Subsequently the same type of critical behavior has been observed for other collapsing fields: the collapse of axisymmetric gravitational wave packets [3], the collapse of spherically symmetric radiative fluids [4]. In all these model problems the critical exponent β turned out to be close to the value originally found by Choptuik $\beta \approx 0.37$, suggesting a universal behavior. However, Maison [5] has shown that for fluid collapse models with an equation of state given by $p=k\rho$ the critical exponent strongly depends on the parameter k.

The second key feature of Choptuik's results is the *universality* of the precisely critical ($p=p^*$) evolution at the threshold of black-hole formation — it was found that the critical solution has a discrete self-similar behavior (discrete echoing with a period Δ).

In this paper we show that it is possible to generalize Choptuik's results for spherically symmetric collapse of an *electrically charged* (complex) massless scalar field [6]. This generalization is not trivial. The invariance of the neutral evolution equations under the rescaling $u \to au$, $r \to ar$, is crucial for the self-similarity of the critical evolution. The introduction of charge (which corresponds to an addition of a parameter with the dimension of length^{-1}) destroys the rescaling invariance and might, therefore, destroy the critical behavior. Using a semiquantitative argument, which is based upon different behavior of the mass and charge under the rescaling $r \to ar$, we argue that the significance and influence of the charge decreases during the evolution and that the critical behavior appears. We provide a numerical evidence for the generalized mass-scaling relation and echoing phenomena for the *charged* situation.

So far, the mass-scaling relation of the black-hole, and the influence of perturbations on the critical evolution itself, have been studied in the context of internal perturbations in the initial conditions, such as a deviation of the field's amplitude from the critical one. It is of interest to compare this phenomenon to other critical phenomenon, such as magnetization phase transition, and to study the behavior of the critical solution under *external* perturbations such as the addition of a cosmological constant Λ. In addition, we examine the effect of varying the charge coupling constant e. We show that the mass of the black hole depends as a power on these parameters. This resembles the situation in the magnetization phase transition in which the magnetization depends as a power on the external magnetic field.

The existence of charged critical behavior stems from the fact that the influence of the charge is weak (and decreasing) near the critical solution. One may wonder whether there is another critical phenomenon in the strongly charged case. Since there is no stationary charged massless scalar field configuration [7] we do not expect to find here a critical behavior of the type discussed by [8] for the Yang-Mills model. While we cannot rule out the existence of another type of critical point, we did not find one while searching numerically the parameter space in the strong charge regime. In all cases calculated we have found that the charged scalar field carried away the excess charge when the initial charge was larger than the initial mass and a finite mass black hole formed. We discuss the strong field regime elsewhere.

The plan of the paper is as follows. In Sec. II we describe the evolution equations. In Sec. III we describe the algorithm and numerical methods. In Sec. IV we describe our discretization and error analysis. In Sec. V we describe our *theoretical* estimates and compare them with our *numerical* results. Sections V A and V B establish both qualitatively and quantitatively the generalization of the mass-scaling relation and echoing phenomena for the *charged* case. In Sec. V C we

study the behavior of the critical evolution under external perturbations. In Sec. V D we study the charge-mass relation for infinitesimal black holes. We show that for $p-p^*\to 0$ the black-hole charge tends to zero more rapidly than its mass and that black holes of infinitesimal mass, which can be created from near-critical evolutions, are neutral, or obey the relation $Q_{\rm BH}\ll M_{\rm BH}$. We conclude in Sec. VI with a brief summary of our results.

II. THE EVOLUTION EQUATIONS

We consider a spherically symmetric charged scalar field ϕ. This is a combination of two real scalar fields ϕ_1, ϕ_2, which are combined into a complex one $\phi=\phi_1+i\phi_2$. The electromagnetic field is described by the potential A, which is defined up to the addition of a gradient of a scalar function. The electromagnetic field tensor F is defined as $2dA$, i.e., $F_{ab}=2A_{[b;a]}$.

The total Lagrangian of the scalar field and electromagnetic field is [9]

$$L=-\frac{1}{2}(\phi_{;a}+ieA_a\phi)g^{ab}(\phi^*_{;b}-ieA_b\phi^*)-\frac{1}{16\pi}F_{ab}F_{cd}g^{ac}g^{bd}, \tag{2}$$

where e is a constant and ϕ^* is the complex conjugate of ϕ.

Varying ϕ, ϕ^* and A_a independently, one obtains [9]

$$\phi_{;ab}g^{ab}+ieA_ag^{ab}(2\phi_{;b}+ieA_b\phi)+ieA_{a;b}g^{ab}\phi=0, \tag{3}$$

and its complex conjugate, and

$$\frac{1}{4\pi}F_{ab;c}g^{bc}-ie\phi(\phi^*_{;a}-ieA_a\phi^*)+ie\phi^*(\phi_{;a}+ieA_a\phi)=0. \tag{4}$$

We express the metric of a spherically symmetric spacetime in the form [1,10]

$$ds^2=-g(u,r)\overline{g(u,r)}du^2-2g(u,r)dudr+r^2d\Omega^2. \tag{5}$$

The radial coordinate r is a geometric quantity which directly measures proper surface area, and u is a retarded time null coordinate. Here $d\Omega^2$ is the two-sphere metric.

Because of the spherical symmetry, only the radial electric field $F^{01}=-F^{10}$ is nonvanishing. This choice satisfies Maxwell's equation

$$F_{[ab;c]}=0. \tag{6}$$

We introduce the auxiliary field h:

$$\phi=\overline{h}\equiv\frac{1}{r}\int_0^r h\,dr. \tag{7}$$

Using the radial component of Eq. (4), we express the charge contained within the sphere of radius r, at a retarded time u, as

$$Q(u,r)=4\pi ie\int_0^r r(\overline{h^*}h-\overline{h}h^*)dr, \tag{8}$$

and the potential as

$$A_0=\int_0^r\frac{Q}{r^2}g\,dr. \tag{9}$$

The energy-momentum tensor of the charged scalar field is [9]

$$T_{ab}=\frac{1}{2}(\phi_{;a}\phi^*_{;b}+\phi^*_{;a}\phi_{;b})+\frac{1}{2}(-\phi_{;a}ieA_b\phi^*+\phi^*_{;b}ieA_a\phi+\phi^*_{;a}ieA_b\phi-\phi_{;b}ieA_a\phi^*)+\frac{1}{4\pi}F_{ac}F_{bd}g^{cd}+e^2A_aA_b\phi\phi^*+Lg_{ab}. \tag{10}$$

The nontrivial Einstein equations are

$$G_{rr}:\quad \frac{2}{r}\frac{g_{,r}}{g}=8\pi\overline{h}_{,r}\overline{h^*}_{,r}, \tag{11}$$

$$G_{ur}:\quad \frac{1}{r^2}\overline{g}\left[\frac{g}{\overline{g}}+r\frac{\overline{g}}{g}\left(\frac{g}{\overline{g}}\right)_{,r}-1\right]=8\pi\left(\frac{1}{2}\overline{gh}_{,r}\overline{h^*}_{,r}+\frac{1}{8\pi}g\frac{Q^2}{r^4}\right). \tag{12}$$

Regularity at the origin requires $g(u,0)=\overline{g(u,0)}$. The boundary condition $h(u,0)=\overline{h(u,0)}$ forces us to integrate the equations outward, and impose the normalization $g(u,0)=\overline{g(u,0)}=1$, which corresponds to selecting the time coordinate as the proper time on the $r=0$ central world line.

The solution at a given r depends only on the solution at $r'<r$. We integrate Eq. (11) and obtain

$$g(u,r)=\exp\left[4\pi\int_0^r\frac{(h-\overline{h})(h^*-\overline{h^*})}{r}dr\right]. \tag{13}$$

Using Eqs. (11) and (12), we obtain, after integration,

$$\overline{g(u,r)}=\frac{1}{r}\int_0^r\left(1-\frac{Q^2}{r^2}\right)g\,dr. \tag{14}$$

In terms of the variable h, the wave equation, Eq. (3), takes the form

$$Dh\equiv h_{,u}-\frac{1}{2}\overline{gh}_{,r}=\frac{1}{2r}(g-\overline{g})(h-\overline{h})-\frac{Q^2}{2r^3}(h-\overline{h})g-\frac{ieQ}{2r}g\overline{h}-iehA_0. \tag{15}$$

Using the characteristic method, we convert the scalar-field evolution equation, Eq. (15), into a pair of coupled differential equations:

$$\frac{dh}{du}=\frac{1}{2r}(g-\overline{g})(h-\overline{h})-\frac{Q^2}{2r^3}(h-\overline{h})g-\frac{ieQ}{2r}g\overline{h}-iehA_0, \tag{16}$$

$$\frac{dr}{du}=-\frac{1}{2}\overline{g}. \tag{17}$$

We solve these equations together with the integral equations (7), (13), (14), (8), and (9). The mass contained within the sphere of radius r at a retarded time u, is

$$M(u,r)\equiv\frac{r}{2}\left(1-\frac{\overline{g}}{g}+\frac{Q^2}{r^2}\right). \tag{18}$$

Using Eqs. (13) and (14), we express M as

$$M(u,r)=\int_0^r\left[2\pi\frac{\overline{g}}{g}(h-\overline{h})(h^*-\overline{h^*})+\frac{1}{2}\frac{Q^2}{r^2}\right]dr+\frac{1}{2}\frac{Q^2}{r}. \tag{19}$$

III. ALGORITHM AND NUMERICAL METHODS

A numerical simulation of the special uncharged case was first performed by Goldwirth and Piran [10]. Gundlach, Price, and Pullin [11] used a version of this algorithm to study the scaling behavior of the mass of the black hole for the special uncharged case. We have used a version of the algorithm of Refs. [10,12], for the neutral case, and we have generalized it for the charged case. However, the methods used in Refs. [10,11] are not accurate enough for a treatment of the critical solution itself, because each successive echo appears on spatial and temporal scales a factor $e^{\Delta}\approx\sqrt{31}$ finer than its predecessor.[1] Our improvements follow Ref. [12] (see below).

To solve numerically Eqs. (16) and (17) we define a radial grid r_n, where $n=1,\ldots,N$. We should emphasize that h is a complex field: $h=h_1+ih_2$, and obtain a set of $3N$ coupled differential equations:

$$\frac{dh_{1n}}{du}=\frac{1}{2r_n}(g_n-\overline{g_n})(h_{1n}-\overline{h_{1n}})-\frac{Q_n^2}{2r_n^3}(h_{1n}-\overline{h_{1n}})g_n+\frac{eQ_n}{2r_n}g_n\overline{h_{2n}}+eh_{2n}A_{0n}, \tag{20}$$

$$\frac{dh_{2n}}{du}=\frac{1}{2r_n}(g_n-\overline{g_n})(h_{2n}-\overline{h_{2n}})-\frac{Q_n^2}{2r_n^3}(h_{2n}-\overline{h_{2n}})g_n-\frac{eQ_n}{2r_n}g_n\overline{h_{1n}}-eh_{1n}A_{0n}, \tag{21}$$

$$\frac{dr_n}{du}=-\frac{1}{2}\overline{g_n}, \tag{22}$$

where g and h satisfy the boundary conditions

$$\overline{g_1}=g_1=1,\quad \overline{h_{11}}=h_{11},\quad \overline{h_{21}}=h_{21}. \tag{23}$$

[1]Our value of Δ is a half of the one used by Choptuik [2]. This definition of the echoing period is based upon the time required for the *physical* quantities, which are quadratic in the derivatives of the scalar field to complete a cycle.

The initial data for the Einstein-scalar-Maxwell equations are just the value of h on the initial data surface, $u=0$, the value of the parameter e, and a numerical choice of the initial position (i.e., the value of r) of each ingoing null lines of the grid.

The algorithm proceeds as follows: first we integrate Eqs. (7), (13), (8), (9), and (14) along r for a fixed u and we obtain in succession the quantities h, g, Q, A_0, and $\overline{g}$. The integration is carried using a three-point Simpson method for unequally spaced abscissas (an evenly spaced grid will not remain so during the evolution [10]). We next use Eqs. (20)–(22), to evolve h and r one time step forward. We solve the $3N$ ordinary differential equations using the fifth-order Runge-Kutta method [13]. This process is iterated as many times as necessary: i.e., until either the field disperses or a charged black hole forms.

The time step Δu is determined so that in each step the change in r_n is less than half the distance between it and the null trajectory r_{n-1}: i.e.,

$$\Delta u<\frac{r_n-r_{n-1}}{\overline{g_n}}. \tag{24}$$

Once a null trajectory arrives at the origin $r=0$, it bounces and disperses along $u=$ const to infinity. The grid point is therefore lost when the light ray hits the origin.

If for a given shell $M>Q$ at some time then it is possible that

$$\overline{e^{2\beta}}(u,r)=1-\frac{2M(u,r)}{r}+\frac{Q^2(u,r)}{r^2} \tag{25}$$

will vanish. We identify the formation of a black hole when there is an r value that satisfies

$$r_{\pm}=M(u,r_{\pm})\pm[M^2(u,r_{\pm})-Q^2(u,r_{\pm})]^{1/2}. \tag{26}$$

In this case $r_{\pm}$ are the horizons of the shell.

As we approach the stage when a black hole forms $\overline{g_n}$ becomes infinite. In our algorithm this means that the step size $\Delta u\to 0$. The numerical approach to the horizon is stopped eventually by an overflow of $\overline{g}$ or underflow of Δu. We can, still, estimate where and when a black-hole horizon appears from the condition $r_+/r\to 1$.

In [11] this method was used to study the scaling behavior of the mass of the uncharged black hole. However, this method is not accurate enough for a treatment of the critical solution itself. The main improvements of our version for the charged case closely resembles that of Ref. [12] where this method was used to study the critical solution for the special neutral case. We will now describe shortly the sources of inaccuracy and the methods that we use to overcome them.

The first source of an inaccuracy arises from the fact that the expressions for the quantities h, g, $\overline{g}$, A_0, and M contains an explicit factor of $1/r$ which diverges at the origin. We overcome this by using a Taylor expansion of h in r:

$$h=h^{(0)}+h^{(1)}r+h^{(2)}r^2+O(r^3). \tag{27}$$

Then we expand the quantities $\overline{h}$, Q, g, $\overline{g}$, A_0, and M in r, where the expansion coefficients are all functions of $h^{(0)}$, $h^{(0)*}$, $h^{(1)}$, $h^{(1)*}$, $h^{(2)}$, and $h^{(2)*}$. Thus, in order to

treat the solution near the origin one needs to find only these coefficients. This is done by fitting the first three values of h to a second-order polynomial: i.e., we solve Eq. (27) for r_1, r_2, and r_3 to obtain $h^{(0)}$, $h^{(1)}$, and $h^{(2)}$. We then use these coefficients to evaluate the values of h, Q, g, $\overline{g}$, and A_0 for the first two values of r. The values of these quantities for other values of r is then determined using a three-point Simpson method for unequally spaced abscissas.

A second source of inaccuracy arises directly from the behavior of the critical solution itself — as the critical solution evolves each successive echo appears on spatial and temporal scales a factor $e^{\Delta}\approx\sqrt{31}$ finer than its predecessor. This problem is solved as follows: Once a null trajectory arrives at the origin $r=0$ it bounces and disperses along $u=$ const to infinity. The grid point is, therefore, lost when the light ray hits the origin. When the number of points decrease by a half we double the number of grid points by introducing new grid points half-way between the old ones and interpolating the values of the variables there. We chose the initial outermost grid point in such a way that this ingoing light ray hits the zero-mass singularity of the critical solution itself. With this choice the doubling decreases the grid spacing in proportion to the spatial structure and the numerical resolution remains the same throughout the evolution.

IV. DISCRETIZATION AND ERROR ANALYSIS

Our grid is highly nonuniform in u if a horizon forms — as we approach the horizon the step size Δu decreases rapidly. Furthermore, even if the grid is evenly spaced initially, it will not remain so during the evolution [10]. However, when we consider two grids in which one has twice the number of grid points as the other, the coarser grid spacing will remain twice the size of the finer grid, when we consider points at the same physical location. We will discuss, therefore, our numerical convergence in terms of the initial grid spacing.

We denote the relative size of the initial grid spacing by l. From condition (24) we see that the spacing Δu is proportional to l. As we have mentioned, we treat Eqs. (16) and (17) as ordinary differential equations in u, and we solve these using a fifth-order Runge-Kutta method [13], the error term is $O(l^6)$.

The calculation of the quantities $\overline{h}$, Q, g, $\overline{g}$, A_0, and M in these equations is nontrivial, and is given by Eqs. (7), (8), (13), (14), (9), and (19), respectively. The integrals are discretized using the three-point Simpson method, the error term in the integration is $O(l^5 f^{(4)})$, where $f^{(4)}$ is the fourth derivative of the integrand f [13].

As we go from one grid to a finer one (i.e., doubling the grid when the number of grid points reach half of the original number) we have to interpolate to obtain the values at the new grid points. The error term in the interpolation is $O(l^4)$.

A critical source of error is the boundary conditions $\overline{g}=g$ and $\overline{h}=h$ at $r=0$ [14]. We treat these boundary conditions by approximating the true value of $h(u,r=0)$ using an interpolation according to Eq. (27), the error term is $O(l^3)$. The situation is even more complicated: The right-hand side of Eq. (16) contains an explicit factor of $1/r$, which in the exact solution is canceled by the boundary conditions.

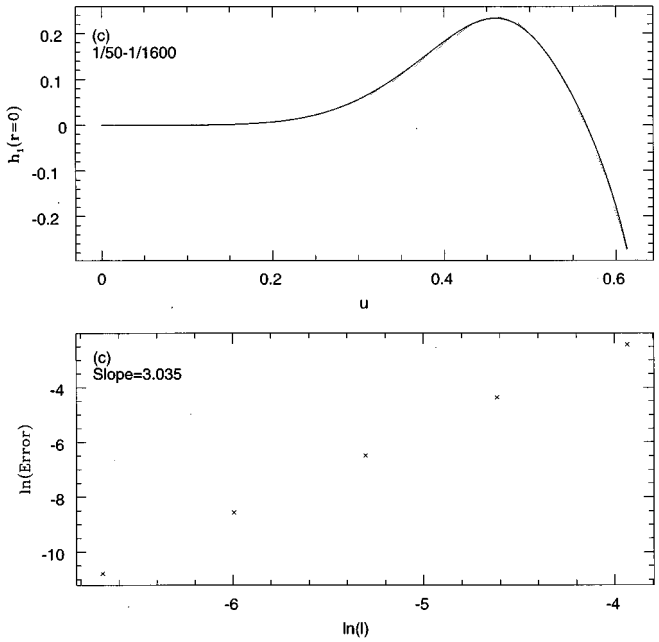

FIG. 1. The convergence of $h(u,r=0)$ with decreasing grid size. The upper panel displays the real part of the scalar field $h_1(u,r=0)$ for different relative grid spacing: 1/1600, 1/800, 1/400, 1/200, 1/100, and 1/50. The numerical errors are so small that the different six curves (for the different grid sizes) actually overlap. The bottom panel displays the convergence of ln of the error (compared to a reference solution with 1600 grid points) as a function of ln of the initial grid size l. The slope is 3.03 ± 0.06. This slope indicates that the error near the origin is largely caused by our handling of the $r=0$ boundary conditions. The initial data are of family (c) with amplitude $A>A^*$ and $e=1$.

The value $h(u,r=0)$ influences all the other physical quantities, and at each and every value of r. It provides, therefore, a good measure of the overall accuracy of the calculations. Three reasons lead to the crucial importance of checking the behavior of the solution near the origin, in order to establish our confidence in the numerical results: (1) The risk of numerical instability caused by the explicit factor of $1/r$; (2) the solution at some value of r depends only on the solution at $r'<r$, so a numerical error in the quantity h near $r=0$, would cause an error at each r, and in all the relevant physical quantities; (3) the critical solution itself, which is the main issue of this work, appears on ever smaller spatial scales during its evolution, leading to the formation of a zero-mass singularity at $r=0$.

Since there are no useful analytical solutions available, we use the numerical solution with the finest resolution (with 1600 grid points) as the reference solution. We compare this solution with the solutions of 800, 400, 200, 100, and 50 grid points. Our error estimate is the square root of the average (over different u values) of the squared difference of $h(u,r=0)$ between a given calculation and the reference one.

Figure 1 displays the error in $h(u,r=0)$. In this figure the initial data are of family (c), with amplitude $A=1.1$ and $e=1$ (see Sec. V for a discussion of initial data). For these initial conditions the gravitational field is strong $(A>A^*)$,

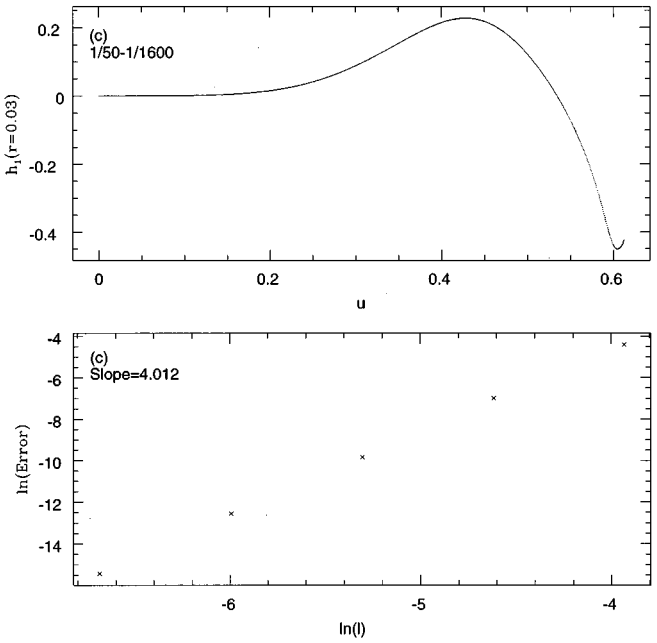

FIG. 2. The convergence of $h(u,r=0.03)$ with decreasing grid size l. The upper panel displays the real part of the scalar field $h_1(u,r=0.03)$ for different relative grid spacing: 1/1600, 1/800, 1/400, 1/200, 1/100, and 1/50. The numerical errors are so small that the different six curves actually overlap. The bottom panel establishes the convergence of the ln of the error (compared to a reference solution with 1600 grid points) as a function of ln of the initial grid size, l. The slope is 4.01 ± 0.05. This slope indicates that in this regime the discretization error due to the interpolation is dominant. The initial data are the same as in Fig. 1.

and the scalar field undergoes a terminal gravitational collapse into a charged black hole. The top part of Fig. 1 establishes visually that the code converges. The bottom part of Fig. 1 shows that the numerical error varies as $l^{3.03\pm0.06}$ as we vary the grid spacing, l. This power indicates that the error near the origin is dominated by the $r=0$ boundary conditions.

We also calculate, in a similar manner, the error in $h(u,r=0.03)$. The top part of Fig. 2 displays again numerical errors that are so small that the different curves (for the different grids) actually overlap. The bottom part of Fig. 2 establishes the stability and convergence of the code: the error varies as $l^{4.01\pm0.05}$. This power indicates that in this regime the discretization error due to the interpolation (used in the grid doubling) is the dominant one.

V. THEORETICAL PREDICTIONS VS NUMERICAL RESULTS

In this section we present our theoretical predictions and numerical results for the gravitational collapse of neutral and charged scalar fields. The numerical results presented arise from a study of several families of solutions, whose initial scalar field $\phi\equiv h$ profiles are listed in Table I:

Families (a) and (b) represent uncharged scalar-field while families (c) and (d) represent charged (complex) scalar field. The amplitude A is the critical parameter p.

TABLE I. Scalar field profiles of several families of solutions.

Family	Form of initial data	e
(a)	$\phi(r)=Ar^2\exp\left[-\left(\frac{r-0.2}{0.1}\right)^2\right]$	0
(b)	$\phi(r)=A\exp(-44r)\cos(100r)$	0
(c)	$\phi(r)=Ar^2\exp\left[-\left(\frac{r-0.25}{0.1}\right)^2\right]+iAr^2\exp\left[-\left(\frac{r-0.15}{0.1}\right)^2\right]$	1
(d)	$\phi(r)=A\exp(44r)\cos(100r)+iA\exp(-75r)\cos(200r)$	1

A. The critical solution

We begin with the critical solution $(p=p^*)$ itself. First, we had to find the value of the critical parameter. Let u^* denote the value of u at which the singularity forms. We define

$$T\equiv-\ln[(u^*-u)/u^*], \tag{28}$$

$$R\equiv r/(u^*-u)=(r/u^*)e^T. \tag{29}$$

In terms of these variables, the critical solution for the neutral case is characterized by a discrete self-similarity [2], i.e., $h(R,T)$ and any other form-invariant quantity such as M/r or dM/dr are periodic functions of T.

Charge destroys the invariance of the neutral evolution equations under the rescaling $u\to au,\ r\to ar$, where a is an arbitrary positive constant. The different scaling of the mass and charge under the rescaling $r\to ar$, suggests however, that the charge will decrease faster than the mass under rescaling. Hence we expect that critically will appear. As the critical solution evolves its structure appears on ever smaller spatial (and temporal) scales. For the neutral case we know that each successive echo appears on spatial and temporal scales which are a factor $a^{-1}\equiv e^{\Delta}\approx\sqrt{31}$ smaller than its predecessor. Under the rescaling $r\to ar$ we have

$$\overline{h}\to\overline{h}, \tag{30}$$

$$g\to g, \tag{31}$$

$$Q\to a^2Q, \tag{32}$$

$$A_o\to aA_o, \tag{33}$$

$$\overline{g}\equiv\overline{g_o}+\overline{g_e}\to\overline{g_o}+a^2\overline{g_e}, \tag{34}$$

$$M\equiv M_o+M_e\to aM_o+a^3M_e, \tag{35}$$

where $\overline{g_o}$ and M_0 are the parts of $\overline{g}$ and M which do not depend on e, and $\overline{g_e}, M_e$ are the additions in the charged case. Since $a<1$ Eqs. (30)–(35) show that if echoing begins then the significance and influence of the charge on the evolution near the origin decreases along the evolution.

Additionally, as the oscillations proceed the scalar field approaches a real function times a constant phase [15]. This leads to an additional decrease in the charge of the form

$$Q\to a^{\xi}Q, \tag{36}$$

$$A_o\to a^{\xi}A_o, \tag{37}$$

$$\overline{g} \equiv \overline{g_o} + \overline{g_e} \rightarrow \overline{g_o} + a^{2\xi}\overline{g_e}, \tag{38}$$

$$M \equiv M_o + M_e \rightarrow aM_o + a^{2\xi}M_e, \tag{39}$$

where ξ is a positive constant (see Sec. V D).

When both effects are combined we find that Q/M decreases approximately with each echo as $Q/M \rightarrow a^{(1+\xi)}(Q/M)$. Looking at the right-hand side of Eq. (16), we find that the various terms scale according to

$$\frac{1}{2r}[g-(\overline{g_o}+\overline{g_e})](h-\overline{h}) \rightarrow \frac{1}{2ar}(g-\overline{g_o})(h-\overline{h}) - \frac{a^{(1+2\xi)}}{2r}\overline{g_e}(h-\overline{h}), \tag{40}$$

$$\frac{Q^2}{2r^3}(h-\overline{h})g \rightarrow \frac{a^{(1+2\xi)}Q^2}{2r^3}(h-\overline{h})g, \tag{41}$$

$$\frac{eQ}{2r}g\overline{h} \rightarrow \frac{a^{(1+\xi)}eQ}{2r}, \tag{42}$$

$$ehA_o \rightarrow a^{(1+\xi)}ehA_o. \tag{43}$$

From here we learn that as the evolution proceeds, the last three terms on the right-hand side of Eq. (16) become smaller relative to the first term by a factor larger than a^2 with each echo. From these arguments we expect to find that for near-critical evolutions the influence of the charge on the evolution should decrease with each echo.

We expect, therefore, that in the precisely critical case ($p=p^*$) and in the limit of an infinite train of echoes, the influence of the charge on the evolution near origin will be ''washed out'' and the solution will reach the Choptuik solution. Since $a \ll 1$ we expect the influence of the charge on the evolution to be negligible even after a small number of echoes. Thus, once echoing begins the solution will approach the neutral one rapidly. Our numerical solution verifies these predictions. Figure 3 shows the quantity $\max(2M/r)$ as a function of T for near-critical evolution of families (a), (b), (c), and (d). The solutions of families (b)-(d) were shifted horizontally but not vertically with respect to family (a) in order that the first echo of each family will overlap the first echo of family (a). After an initial phase of evolution the quantity $\max(2M/r)$ settles down to a periodic behavior in T. The period is $\Delta \approx 1.73$ which corresponds to previous numerical results found by Choptuik [2] for the neutral case.

Figure 3 also provides a numerical evidence for the *universality* of the strong-field evolution of a critical configuration. In order to verify that this universality exists for each and every value of r we display in Fig. 4 profiles of M/r as a function of R for T values at which the quantity $\max(2M/r)$ reaches its maximum as a function of T. (It should be emphasized that Fig. 4 is composed of *16* profiles — 4 for each family.) The close similarity of the profiles illustrates two important properties:

(1) For each family by itself, the critical solution is periodic. Each successive echo appears on spatial and temporal scales a factor $e^{\Delta} \approx \sqrt{31}$ finer than its predecessor.

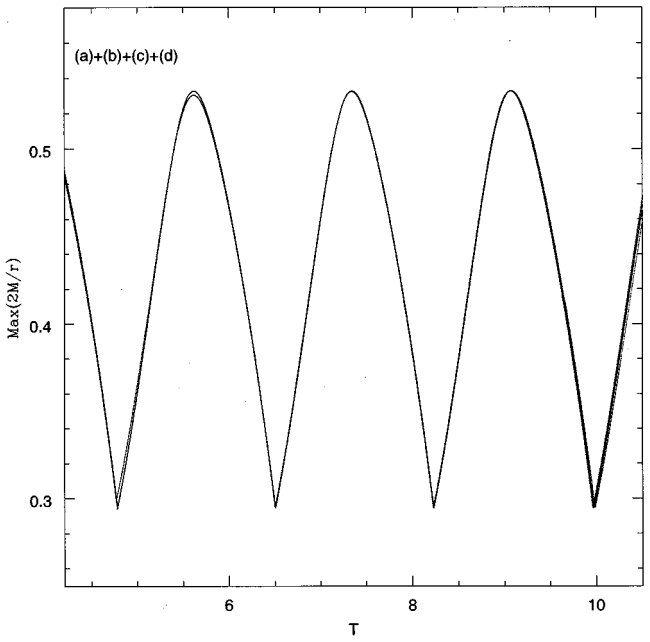

FIG. 3. Illustration of the universality of the critical evolution in the gravitational collapse of a charged (complex) scalar field. max $(2M/r)$ is plotted as a function of the logarithmic time T for the neutral families (a), (b) and for the charged families (c) and (d) (from near-critical evolutions). The curves were shifted horizontally (but not vertically) in order to overlap the first echo of each family with the first echo of family (a). After an initial evolution the quantity $\max(2M/r)$ settles down to a periodic behavior in T with a period $\Delta \approx 1.73$, which corresponds to the one found by Choptuik for the neutral case.

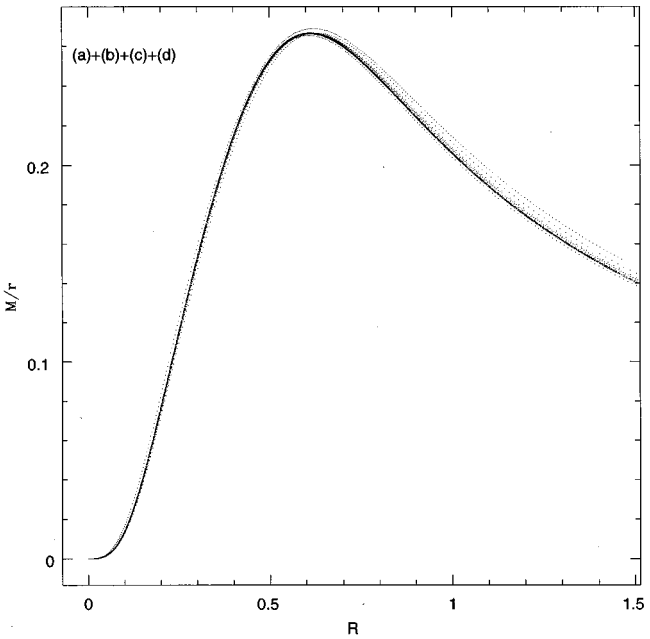

FIG. 4. The profiles of M/r for each of the four families, as a function of the logarithmic coordinate R in those times at which the quantity $\max(2M/r)$ reaches its maximum as a function of T. (It should be emphasized that this figure is composed from 16 profiles – 4 for each family.)

(2) The close similarity of the profiles illustrates the uniqueness of the critical solution and its independence of the initial profile and charge.

B. Scaling behavior of the black-hole mass

We turn now to the power-law dependence of the black-hole mass. The critical solution by itself does not yield the black-hole scaling relation. We should perturb the critical initial conditions. This would lead to a dynamical instability — a growing deviation from the critical evolution towards either subcritical dissipation or supercritical charged black-hole formation. To describe the run away from the critical evolution we consider a perturbation mode with a power-law dependence $\lambda(u^*-u)^{-\alpha}$ [4,5], where $\lambda \propto (p-p^*)$. Assume the range of validity of the perturbation theory is restricted to some maximal deviation σ from the critical evolution, i.e., the evolution is approximately self-similar until the deviation from the critical solution reach the value σ. From here on the evolution is outside the scope of the perturbation theory — there is subcritical dissipation of the field or supercritical black-hole formation. In either case, the evolution from this stage on has no self-similar character.

We consider a perturbation in the initial conditions that develops into a charged black hole. The time $u_\sigma(p-p^*)$ required to reach a deviation σ is given by the relation

$$\lambda(u^*-u_\sigma)^{-\alpha}=\sigma. \tag{44}$$

Of course, a larger initial perturbation requires a smaller time u_σ — the horizon is formed sooner. The logarithmic time T_σ is given by

$$T_\sigma=-\frac{1}{\alpha}\ln(p-p^*)+b_k, \tag{45}$$

where b_k depends on σ and u^*.

In a following paper [6,16] we prove that one should add a *periodic* term $F[\ln(p-p^*)]$ to T_σ to obtain the total logarithmic time $T_{\rm BH}$ until the horizon formation. The *periodic* term $F[\ln(p-p^*)]$ has a universal period $\varpi=\Delta/\beta$. Thus, the complete dependence of $T_{\rm BH}$ on the critical separation $p-p^*$, for both the neutral and the charged cases, is given by

$$T_{\rm BH}=-\frac{1}{\alpha}\ln(p-p^*)+F[\ln(p-p^*)]+b_k. \tag{46}$$

Figure 5 displays $-T_{\rm BH}$ as a function of $\ln(a)$, where $a=(A-A^*)/A^*$. The calculated points are well fit by a straight line whose slope is $1/\alpha\approx 0.37$. This is consistent with relation (46).

The exponent α is related to β, the critical exponent that describes the power-law dependence of the black-hole mass. We define $M^{(n)}$ as the mass after n echoes. Following this definition we define

$$M^{(o)}=M_o^{(o)}+M_e^{(o)}\equiv(1+C)M_o^{(o)}, \tag{47}$$

where M_o is the part of M which does not depend on e and M_e is the charge contribution in the charged case. From Eqs. (35) and (39) it follows that

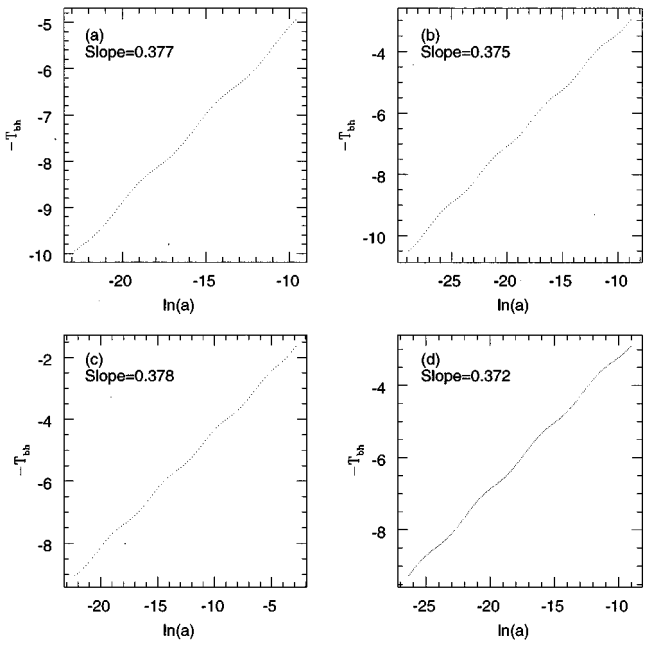

FIG. 5. The logarithmic time of a black-hole formation, plotted as $-T_{\rm BH}$ as a function of $\ln(a)$ [where $a=(p-p^*)/p^*$] for the four families. The average slope is $1/\alpha\approx 0.37$, which is consistent with relation (46). The oscillations seen above the straight line are physical [6].

$$M^{(n)}=M_o^{(o)}e^{-n\Delta}+CM_o^{(o)}e^{-(3+2\xi)n\Delta}. \tag{48}$$

We substitute Eq. (45) into Eq. (48) and, assuming that $M^{(o)}$ and C do not depend on $p-p^*$, obtain

$$\ln M_{\rm BH}=c_k+(1/\alpha)\ln(p-p^*)+O[e^2(p-p^*)^{2\beta(1+\xi)}], \tag{49}$$

where c_k is a family-dependent constant. Using the usual definition of the mass critical exponent, β: $M_{\rm BH}\propto(p-p^*)^\beta$, we find that $\beta=1/\alpha$.

Thus, according to the perturbation theory, the critical exponent β describes both the scaling relation of the black-hole mass and the deviation rate from the critical evolution caused by perturbations. In a following paper[2] [6,16] we show that one should add a periodic term $\Psi[\ln(p-p^*)]$ with a universal period $\varpi=\Delta/\beta$ to the scaling relation (49).

Figure 6 displays $\ln(m)$ as a function of $\ln(a)$, where m is the normalized black-hole mass in units of the initial mass in the critical solution. The points are well fit by a straight line whose slope is $\beta\approx 0.37$ which is consistent with $\beta=1/\alpha$. The measured value of the critical exponent β in the charged case agrees with the one of Choptuik for neutral collapse. Thus, Fig. 6 presents a generalization of the mass-scaling phenomenon for the *charged* case.

In the neutral case the black-hole mass is proportional to its radius and either the mass or the radius could be the physical order parameter. In the charged case the black hole radius equals $M+(M^2-Q^2)^{1/2}$ and in general it is no longer proportional to M. However, as we approach the critical so-

[2]See also [17].

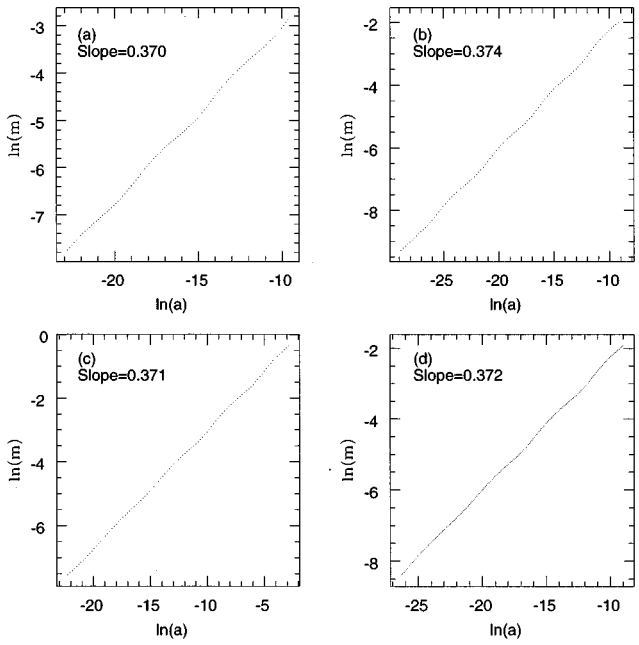

FIG. 6. Scaling of the black-hole mass: $\ln(m)$ vs $\ln(a)$ for the neutral families (a), (b) and for the *charged* families (c) and (d). m is the normalized black-hole mass in units of the initial mass in the critical solution. The points are well fit by a straight line whose slope is $\beta \approx 0.37$ which is consistent with $\beta = 1/\alpha$. The measured value of the critical exponent β in the charged case agrees with the one previously found for the neutral case. The oscillations above the straight line are physical [6,16,17].

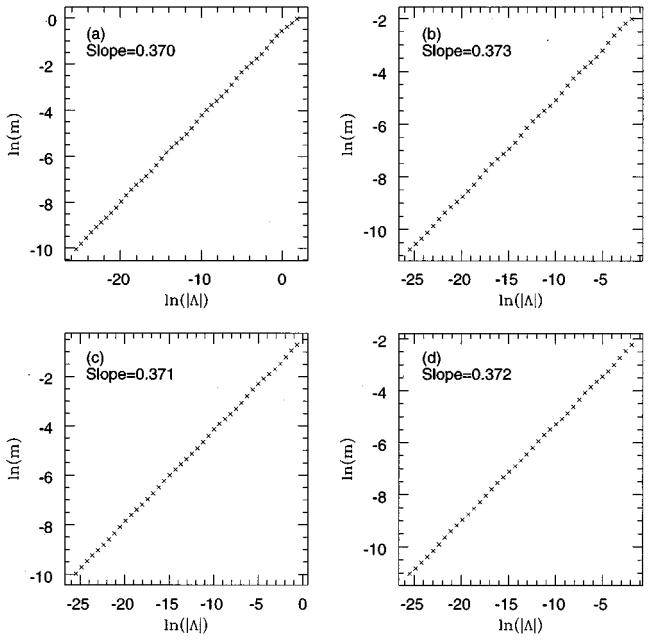

FIG. 7. Power-law dependence of the black-hole mass on the cosmological constant. $\ln(m)$ is plotted vs $\ln(-\Lambda)$ for the four families. The points are well fit by a straight line whose slope is $1/\delta$, where $1/\delta \approx \beta$. This provides an evidence for the power-law dependence of the black-hole mass on external parameters. The initial conditions are for $A = A^*$.

lution, the significance of the charge decreases with each echo. The quantity Q/M becomes smaller as the black-hole mass gets smaller and it is impossible to distinguish between the two possibilities.

C. External perturbations to the critical solution

So far, the mass-scaling relation of the black hole, and the influence of perturbations on the critical evolution itself, have been studied in the context of internal perturbations in the initial conditions, such as a deviation of the field's amplitude from the critical one. It is of interest to study the behavior of the critical solution under *external* perturbations. In particular, we have studied the behavior of the critical evolution under an addition of a cosmological constant Λ. This is analogous to the addition of an *external* magnetic field to a system of magnetic moments and studying the magnetization dependence on the strength of the external field exactly at the critical temperature T_c (at $T = T_c$ the magnetization is zero without an external magnetic field, just as the zero-mass singularity for $A = A^*$ and $\Lambda = 0$). The analogy arises from the fact that in both cases the *external* perturbation, magnetic field or a cosmological constant, forces the order parameter to have a nonzero value at $T = T_c$ or at $A = A^*$, correspondingly. We have considered also the effect of variation of the charge coupling constant, e on the system.

The external perturbation, Λ (or a variation of e), is expected to yield a dynamical instability — a growing deviation from the critical evolution toward either subcritical dissipation or supercritical black-hole formation. The unperturbed solution forms a zero-mass singularity. The perturbation could lead to a finite mass black hole and we examine the dependence of this mass on the *external* parameters: Λ or e.

1. Cosmological constant Λ

We first examine the effect of an addition of a cosmological constant to a critical solution. The amplitude was set to the critical value A^* (for $\Lambda = 0$). We then add a cosmological-constant, Λ, and study its influence on the evolution. $\Lambda > 0$ led to a dissipation of the critical solution and, on the other hand, $\Lambda < 0$ gave rise to a finite-mass black-hole formation.

For $\Lambda \neq 0$, the generalization of Eq. (14) is

$$\overline{g(u,r)} = 1/r \int_0^r [1 - (Q^2/r^2) - \Lambda r^2] g dr. \tag{50}$$

In addition, one should add the term

$$-\Lambda/2 r g (h - \overline{h}), \tag{51}$$

to the right-hand side of Eq. (16). Evidence for the *universality* and the power-law dependence of the black hole mass on the *external* parameter Λ is shown in Fig. 7 which displays $\ln(m)$ as a function of $\ln(-\Lambda)$ for critical initial-conditions $(A = A^*)$. The points are well fit by a straight line: i.e.,

$$M_{\mathrm{BH}}|_{p=p^*} \propto (-\Lambda)^{1/\delta}. \tag{52}$$

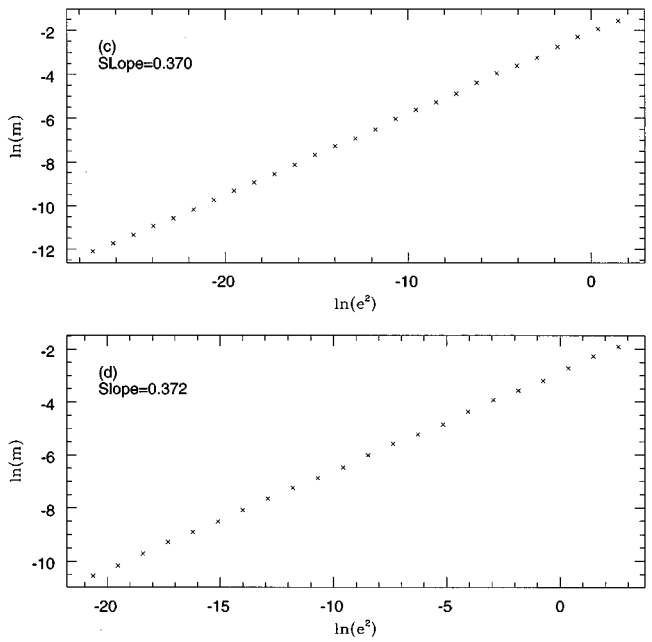

FIG. 8. Power-law dependence of the black-hole mass on charge coupling constant e. $\ln(m)$ is plotted vs $\ln(e^2)$ for the charged families (c) and (d). The points are well fit by a straight line whose slope is $\gamma/2 \approx \beta$. The initial conditions are for $A = A^*$.

A priori there is no reason to assume a specific value of δ. However, we find numerically that $1/\delta \approx \beta$. This shows that the addition of a cosmological constant shifts the critical parameter in a relatively simple way:

$$M_{\mathrm{BH}} \propto (p - p^* - s_k \Lambda)^{\beta}, \tag{53}$$

where s_k is a family-dependent constant.

2. Variation of the charge coupling constant e

We consider now the two charged families, (c) and (d), for the case where $e = 0$. The amplitude was first set to its critical value A^* for the families (c) and (d), with $e = 0$. For $e = 0$, the initial conditions represent an uncharged complex scalar field. We then turn on the charge — we add a charge coupling constant e, and study its influence. We examine the black-hole mass as a function of the charge coupling constant e (keeping $A = A^*$). The numerical results are shown in Fig. 8, which displays $\ln(m)$ as a function of $\ln(e^2)$. The points are well fit by a straight line: i.e.,

$$M_{\mathrm{BH}}\big|_{p=p^*} \propto |e|^{\gamma}. \tag{54}$$

Once more we find the simple relation $\gamma \approx 2\beta$, which leads to the general formula

$$M_{\mathrm{BH}} \propto (p - p^* + S_k e^2)^{\beta}, \tag{55}$$

with another family dependent constant, S_k.

A more detailed picture of the formation of a charged black hole near the phase transition is given by considering the full two-dimensional phase space $p - p^*$ and e^2. This was done both for subcritical $(A < A^*)$ initial conditions and for supercritical $(A > A^*)$ initial conditions, close to the phase transition $(|A - A^*| \ll A^*)$. Subcriticality and supercriticality are defined here relative to a neutral configuration with $e = 0$. Figure 9 displays the dependence of the black-

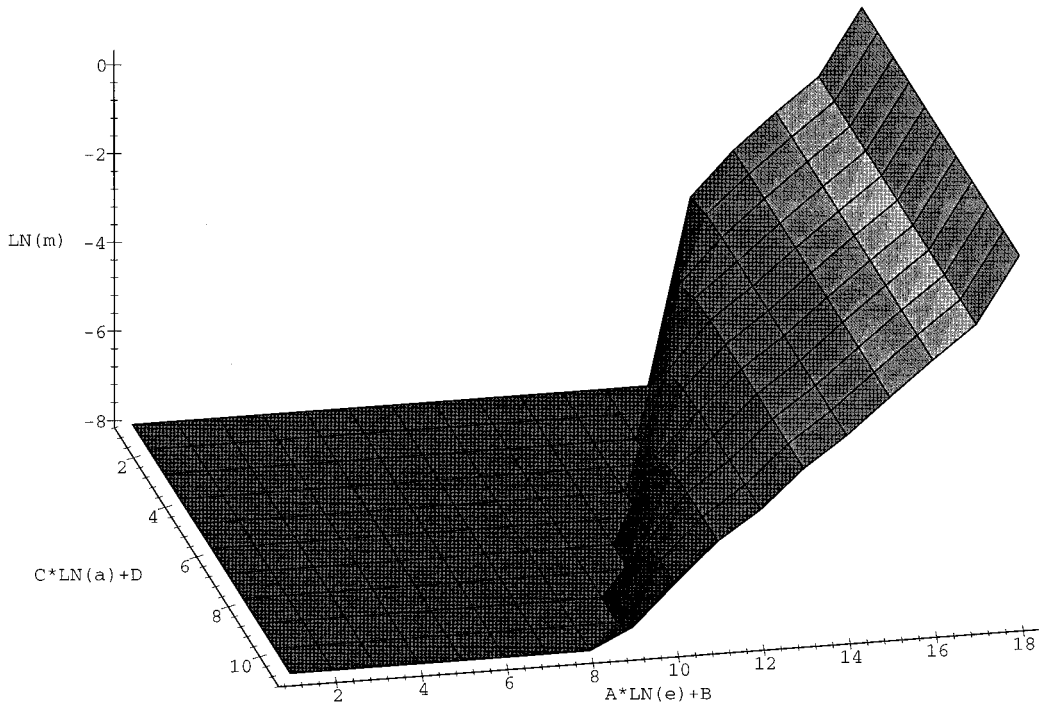

FIG. 9. The black-hole mass, $\ln(m)$, as a function of $\ln(a) = \ln[(A^* - A)/A^*]$ and $\ln(e)$, for subcritical initial conditions $(A < A^*)$. The charge opposes gravitation but the electromagnetic energy also contributes to the gravitational binding and leads to the formation of a black hole even from subcritical initial conditions. Black holes do not form in the flat regime. A, B, C, and D are normalization constants: $A = 1$, $B = 16$, $C = -1$, $D = -11.061$.

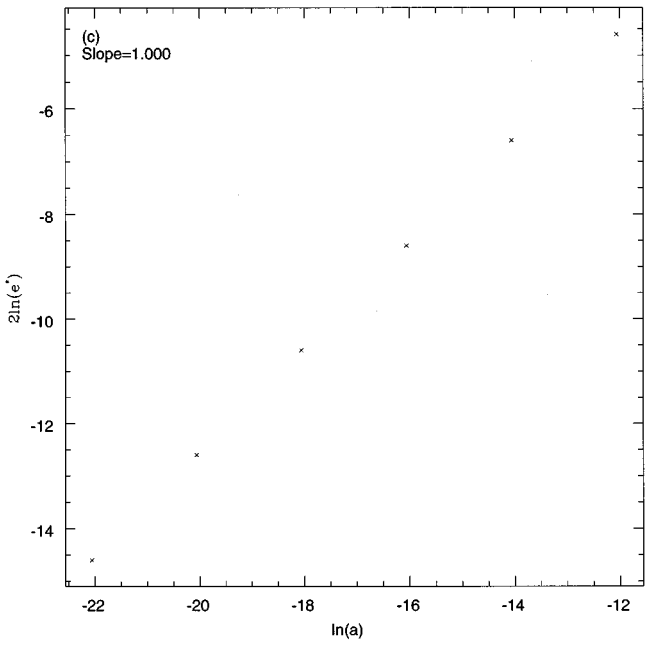

FIG. 10. Power-law dependence of the critical charge coupling constant e^* on the critical separation $|A-A^*|$, for subcritical ($A<A^*$) initial conditions. e^* is the minimal charge coupling constant needed for black-hole formation from subcritical initial conditions.

hole mass which forms from subcritical initial conditions ($A<A^*$) as a function of $\ln(a)$ and $\ln(e)$, for family (c). It shows that the addition of charge can lead to a black-hole formation from subcritical initial conditions ($A<A^*$). Charge opposes gravitation but the electromagnetic energy density also contributes to the gravitational binding, and by doing so it permits the formation of a black hole even from subcritical initial conditions.

The critical charge coupling constant e^*, needed to obtain a black hole from subcritical initial conditions, is well described by a power-law dependence on critical separation $|A-A^*|$:

$$e^* \propto (p^*-p)^{\epsilon}, \tag{56}$$

where $\epsilon=0.5$ (see Fig. 10). This confirms relations (55) derived earlier.

Figure 11 displays the dependence of the black-hole mass formed from supercritical initial conditions ($A>A^*$) as a function of $\ln(a)$ and $\ln(e)$, for family (c). Near the phase transition, the larger the critical separation $p-p^*$ and the charge coupling constant e, the larger is the black-hole mass. The slope of the right edge of the surface is β, which is consistent with Eq. (49). The slope of the left edge of the surface is 2β, which is consistent with Eq. (54). The overall shape is consistent with Eq. (55).

The tight relation between the various critical-exponents β, δ, and γ, which all describe the *instability* of the critical evolution under a variety of different *perturbations*, is a strong evidence supporting the conjecture that there exists one mechanism which can explain the power-law dependence of the black-hole mass on the various parameters, both for internal perturbations in the initial conditions and for external perturbations as well.

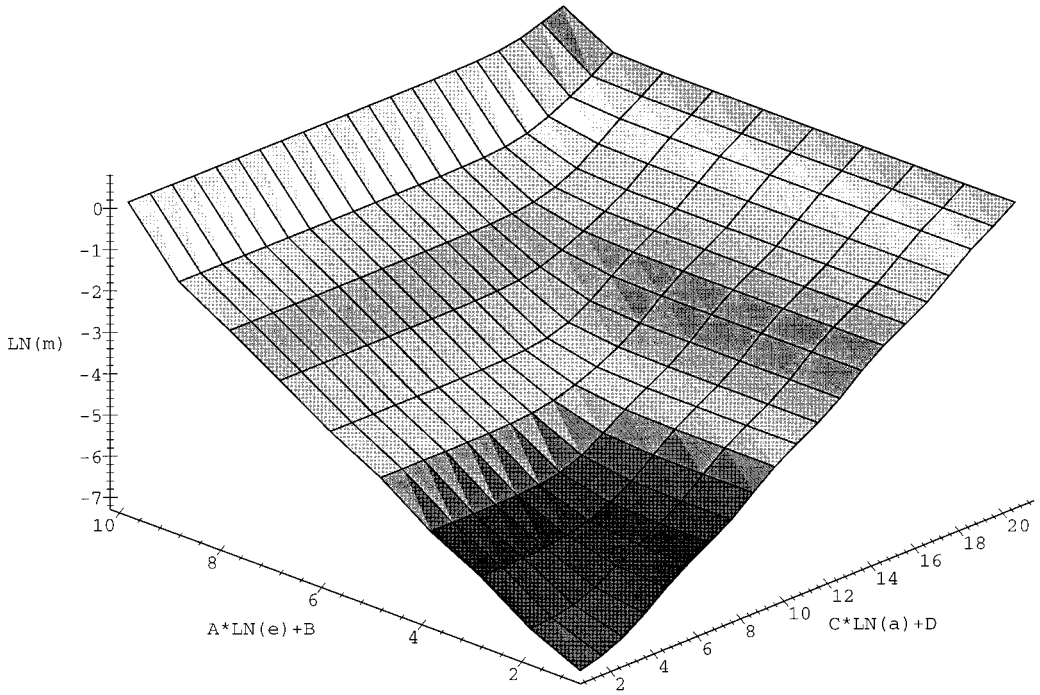

FIG. 11. The black-hole mass, $\ln(m)$, is plotted as a function of $\ln(a)=\ln[(A-A^*)/A^*]$ and $\ln(e)$, for supercritical initial conditions ($A>A^*$). Near the phase transition, the larger the critical separation $p-p^*$ and the charge coupling constant e, the larger is the black-hole mass. The slope of the right edge of the surface is β, which is consistent with Eq. (49). The slope of the left edge of the surface is 2β, which is consistent with Eq. (54). A, B, C, D are normalization constants: $A=1$, $B=8$, $C=1$, $D=23.061$.

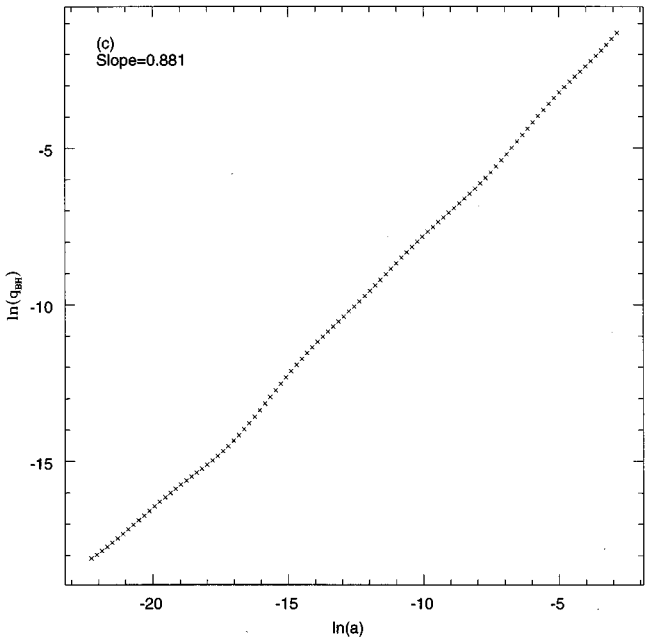

FIG. 12. Illustration of the conjectured charge-scaling relation (58). $\ln(q_{\rm BH})$ is plotted vs $\ln(a)$ for near-critical black holes, where $q_{\rm BH}$ is the normalized black-hole charge in units of the initial charge in the critical solution. Data from the charged family (c) is shown. The points are well fit by a straight line whose slope η obeys the relation $\eta>2\beta$. Thus for $p-p^*\to 0$ the black-hole charge tends to zero more rapidly than its mass.

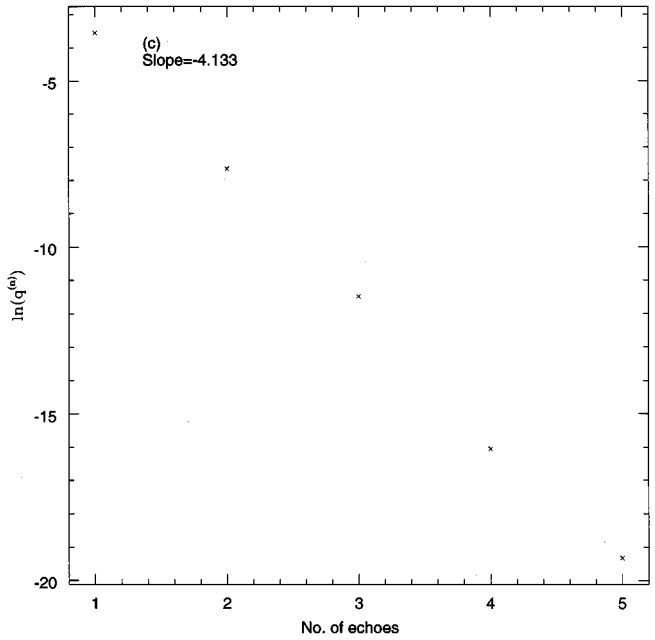

FIG. 13. The decrease of the charge with each echo during the critical evolution. The points are well fit by a straight line whose slope is $-(2+\xi)\Delta\approx -4.133$.

D. The charge-mass relation for black holes

We have shown in Sec. V A that the black-hole charge tends to zero faster than its mass for $p-p^*\to 0$. We demonstrate now that $Q\to 0$ as a power law with a critical exponent larger than 2β (see also [15] for an independent analysis of this problem). Define $Q^{(n)}$ as the charge after n echoes. From Eqs. (32) and (36) it follows that

$$Q^{(n)}=Q^{(0)}e^{-(2+\xi)n\Delta}. \tag{57}$$

Substituting Eq. (45) into Eq. (57) and assuming that $Q^{(0)}$ does not depend on $p-p^*$ we obtain

$$\ln|Q_{\rm BH}|=(2+\xi)\beta\ln(p-p^*)+d_k, \tag{58}$$

where d_k is a family-dependent constant.

From this analytic argument we deduce two conclusions: (1) The black-hole charge is expected to have a power-law dependence on critical separation $p-p^*$, where the critical exponent η is closely related to the critical exponent β of the mass according to $\eta=(2+\xi)\beta$; (2) the black-hole charge tends to zero with $p-p^*$ more rapidly than its mass.

Figure 12 displays $\ln q_{\rm BH}$ as a function of $\ln(a)$ for near-critical black holes, where $q_{\rm BH}$ is the normalized black-hole charge in units of the initial charge in the critical solution. The points are well fit by a straight line whose slope is $\eta\approx 0.88$. This is consistent with relation (58).

Another way to determine the value of η is directly from Eqs. (57) and (58). Figure 13 displays $\ln q^{(n)}$ as a function of n, the number of echoes, along the critical solution. The slope is $-(2+\xi)\Delta\approx -4.133$. Using $\Delta\approx 1.73$ and $\beta\approx 0.37$ we find $\eta\approx 0.883$, in agreement with the prediction, $\eta=0.883\pm 0.007$, of Gundlach and Martin-Garcia [15].

The data shown in Figs. 12 and 13 come from the charged family (c). For family (d) we have found that in general the charge increases as the critical separation $p-p^*$ increases although this correlation is not well described by a power-law dependence. The reason for this probably arises from the initial phase of the evolution. The initial data in this family contains rather narrow alternating layers of positive and negative charge whose relative magnitude depends on p. The initial evolution that precedes the critical oscillations could lead therefore, depending on p to drastically different total charge. Consequently, the assumption that $Q^{(0)}$ does not depend on $p-p^*$ breaks down for this configuration. Despite this, our numerical results qualitatively confirm our prediction — the black-hole charge tends to zero with $p-p^*$ faster than its mass. From here we conclude that black-holes with infinitesimal mass, which, according to this mechanism, can be created from near-critical evolutions, are neutral, or obey the relation $Q_{\rm BH}\ll M_{\rm BH}$.

VI. SUMMARY AND CONCLUSIONS

We have studied the spherical gravitational collapse of a charged (complex) scalar field. The main issue considered is the generalization of the critical behavior, originally discovered by Choptuik for neutral fields, for the general *charged* case. We have shown that the significance and influence of the charge decreases during the evolution and consequently the critical behavior appears. As $p-p^*\to 0$ the black-hole charge tends to zero faster than its mass, i.e., $Q_{\rm BH}/M_{\rm BH}\to 0$ as $p\to p^*$. Thus, we conjecture that black holes of infinitesimal mass, which can be created from near-critical evolutions, are neutral, or obey the relation $Q_{\rm BH}\ll M_{\rm BH}$. Consequently, we find both the mass scaling

relations for supercritical solutions and the echoing phenomenon for the critical solution. We show that the charge of the black hole also depends, as a power law on the separation from criticality. The critical exponent is $\eta > 2\beta$ [15].

We have also studied the response of the critical solution to *external* perturbations. In particular, we have studied the behavior of the critical evolution under the addition of a cosmological constant Λ, and the addition of charge coupling constant e to a neutral critical configuration of a complex scalar field. We have found a power-law dependence of the black-hole mass on *external* parameters Λ and e. External perturbations can vary the critical parameter and can lead to black hole formation from what was subcritical ($p < p^*$) initial conditions. The critical charge coupling constant e^*, which is needed to form black holes from subcritical initial conditions, is well described by a power-law dependence on critical separation $p^* - p$.

The tight relation between the various critical exponents β, δ, and γ, which all describe the *instability* of the critical evolution under a variety of different *perturbations*, is a strong evidence supporting the conjecture that there exists one mechanism which can explain the power-law dependence of the black-hole mass on the various parameters, both for internal perturbations and for external ones.

ACKNOWLEDGMENTS

We thank Shai Ayal for technical help, Amos Ori for helpful discussions, and Carsten Gundlach for critical remarks. This research was supported by a grant from the US-Israel BSF and a grant from the Israeli Ministry of Science.

[1] D. Christodoulou, Commun. Math. Phys. **105**, 337 (1986).
[2] M. W. Choptuik, Phys. Rev. Lett. **70**, 19 (1993).
[3] A. M. Abrahams and C. R. Evans, Phys. Rev. Lett. **70**, 2980 (1993).
[4] G. R. Evans and J. S. Coleman, Phys. Rev. Lett. **72**, 1782 (1994).
[5] D. Maison, Phys. Lett. B **366**, 82 (1996).
[6] S. Hod, M.Sc. thesis, The Hebrew University, Jerusalem, 1995.
[7] Ph. Jetzer and J. J. Van der Bij, Phys. Lett. B **227**, 341 (1989).
[8] M. W. Choptuik, T. Chmaj, and P. Bizon, Phys. Rev. Lett. **77**, 424 (1996).
[9] S. W. Hawking and G. F. R. Ellis, *The Large Scale Structure of Space Time* (Cambridge University Press, Cambridge, England, 1973).
[10] D. S. Goldwirth, and T. Piran, Phys. Rev. D **36**, 3575 (1987).
[11] C. Gundlach, R. H. Price, and J. Pullin, Phys. Rev. D **49**, 890 (1994).
[12] D. Garfinkle, Phys. Rev. D **51**, 5558 (1995).
[13] W. H. Press, S. A. Teukolsky, W. T. Vetterling, and B. P. Flannery, *Numerical Recipes in Fortran: The Art of Scientific Computing*, 2nd ed. (Cambridge University Press, Cambridge, England, 1992).
[14] M. W. Choptuik, D. S. Goldwirth, and T. Piran, Class. Quantum Grav. **9**, 721 (1992).
[15] C. Gundlach and J. M. Martin-Garcia, Phys. Rev. D **54**, 7353 (1996).
[16] S. Hod and T. Piran, Phys. Rev. D **55**, R440 (1997).
[17] C. Gundlach, Phys. Rev. D **55**, 695 (1997).